JOURNAL OF MAGNETIC RESONANCE, Series A **118,** 202–213 (1996)
ARTICLE NO. 0028

Lineshape Variations of a Spin-$\frac{1}{2}$ Nucleus Coupled to a Quadrupolar Spin Subjected to RF Irradiation

N. MURALI* AND B. D. NAGESWARA RAO

Department of Physics, Indiana University–Purdue University Indianapolis, 402 North Blackford Street, Indianapolis, Indiana 46202-3273

Received June 26, 1995; revised October 31, 1995

In this paper, the lineshape variations in the multiplet structure of a spin-$\frac{1}{2}$ nucleus I (^{13}C) scalar coupled to a quadrupolar spin S (^{2}H) as a function of the strength of the irradiating radiofrequency field applied in the vicinity of the S-spin resonance and of the relaxation times of the latter are presented. These lineshapes were simulated using an exact theoretical treatment based on the solution of the complete-density-matrix equations (including both coherent and incoherent parts) in the presence of RF irradiation of spin S. The relaxation mechanisms for the spin system include chemical-shift anisotropy (CSA) for spin I, quadrupolar interaction for spin S, and the mutual dipole–dipole interaction between I and S. The simulations incorporate interference effects arising from the simultaneous presence of these tensor interactions of the same order, which cause both lineshape variations as well as dynamic frequency shifts. The RF field strength of the irradiation was varied over a wide range, and the two cases of (i) complete and (ii) incomplete ''washing out'' of the spin coupling between the nuclei are considered separately. The simulations illustrate the dependence of the spectrum of spin I on various parameters such as the value of the scalar coupling constant, the quadrupolar relaxation times, and the irradiation strength in commonly realized experimental context. In addition, a simpler theory for the case of completely washed out scalar coupling in which the scalar interaction is treated exclusively as a relaxation process is presented in the Appendix. The procedure given in this paper is applicable to lineshape calculations for any spin-$\frac{1}{2}$–spin-1 coupled system.

INTRODUCTION

Recent developments in high-resolution multinuclear multidimensional NMR methods for the determination of macromolecular structure involve extensive use of selective, semiselective, or uniform ^{13}C, ^{15}N, and ^{2}H labeling of the macromolecule (*1, 2*). Such labeled spin systems often contain fragments with a spin-$\frac{1}{2}$ and spin-1 directly bonded to each other such as ^{13}C–^{2}H, ^{13}C–^{14}N, ^{15}N–^{2}H, and ^{1}H–^{14}N. All these spin pairs have a *J*-coupling interaction between them. However, the spin–spin splitting is partially or totally ''washed out'' by the rapid quadrupolar relaxation of the spin-1 (*3, 4*). There is usually some residual line broadening in the observed spectrum of the spin-$\frac{1}{2}$ nucleus. Since one of the motivations behind isotope editing is to enhance resolution, and thereby facilitate structure determinations of macromolecules of larger size (*1, 2, 5–8*), strategies have been used to minimize this residual linewidth by the use of radiofrequency irradiation in the vicinity of the resonance of the spin-1 nucleus (*9*).

The effect of such an RF perturbation has several components, the relative importance of which depends on the relaxation and spectral parameters of the spin system (*10, 11*). If the *J* coupling is only incompletely averaged by the relaxation of the quadrupolar nucleus, the RF irradiation may be used to complete the spin decoupling, and thereby cause line narrowing. On the other hand, even if the *J* coupling is completely washed out by the quadrupolar relaxation, the RF perturbation may be used to modify the spectral densities contributing to the linewidth of the spin-$\frac{1}{2}$ resonance, and this too leads to line narrowing especially in the long-correlation-time limit. The role of RF perturbation in these two cases is clearly delineable; in the case of decoupling, the coherent interplay between the RF and *J*-coupling interactions is the primary factor, and, in the other case, the line narrowing of the fully decoupled resonances is an example of manipulating the relaxation effects by the coherent RF perturbation typically manifest in rotating-frame relaxation experiments such as the CAMELSPIN (*12*) or ROESY experiments (*13*). It is, nevertheless, possible to cast a unified formulation in which both these phenomena can be seen under appropriate physical conditions. One of the motivations of this paper is to provide such a formalism along with computer-simulated lineshapes to illustrate the effects. The theory and simulations provide a basis for optimizing the strengths of the RF field to be used in the experiments.

* Present address: Center for Interdisciplinary Magnetic Resonance, National High Magnetic Field Laboratory, 1800 E. Paul Dirac Drive, Tallahassee, Florida 32310.

1064-1858/96 $18.00

Furthermore, these results help to clarify some of the confusion in the literature on the subject which appears to have led to the use of RF field strengths far in excess of those necessary to obtain line narrowing in the spectra.

The line narrowing generated through the use of RF fields is yet another example of a variety of experiments in NMR that use RF fields to manipulate the spin Hamiltonian of the system. There are a number of examples of using RF fields to effectively alter the coherent (or spectral) part of the Hamiltonian such as spin decoupling and cross polarization (*14*). Experiments that modify the incoherent (or relaxation) part of the spin Hamiltonian are often not possible and are less common. Recent experiments designed to select relaxation pathways to retain specific pair-wise dipolar interactions and suppress spin-diffusion effects are examples of tailoring the relaxation Hamiltonian without altering the spectral Hamiltonian (*15, 16*). In a number of situation such as the line-narrowing experiments considered here, an exact theoretical treatment requires solution of the complete-density-matrix equations (including both coherent and incoherent parts) in the presence of the RF perturbation. Such a procedure for the calculation of lineshapes for a spin-$\frac{1}{2}$ (^{13}C) nucleus coupled to a spin-1 (^{2}H) nucleus relaxing through quadrupolar interaction in the presence of a strong RF irradiation of the latter spin is given below. The theory is used to simulate lineshapes over a range of RF field strengths inclusive of the cases of complete and incomplete washing out of the spin coupling between the nuclei. In the Appendix, a simpler theory for the case of completely washed-out scalar coupling, in which the scalar interaction is treated exclusively as a relaxation process, is presented.

For the relaxation of the spin system, three mechanisms are considered: the chemical-shift anisotropy (CSA) of spin I ($\frac{1}{2}$), quadrupolar interaction for spin S (1), and their mutual dipolar interactions. Since all these are tensor interactions of rank 2, interference terms can arise between relaxation mechanisms such as, dipolar–quadrupolar interaction and dipolar–CSA cross correlations (*4, 17*). So-called dynamic frequency shifts arising from the imaginary part of the spectral densities of the relaxation mechanisms can also occur (*4, 18–20*). These effects are also included in the present formulation. The procedure in this paper is, therefore, applicable to lineshape calculations for any spin-$\frac{1}{2}$–spin-1 coupled system under a variety of commonly realized experimental conditions.

THEORY

The density-matrix method is convenient for the calculation of the lineshape variations in the multiplet structure of a spin-$\frac{1}{2}$ nucleus I as a function of the relaxation times of a quadrupolar spin S and of the strength of the irradiating RF field applied in the vicinity of the S-spin resonance. The equation of motion for the spin density matrix $\boldsymbol{\sigma}$ is given by

$$\frac{d\boldsymbol{\sigma}}{dt} = -i[\mathcal{H}_0(t) + \mathcal{H}_J + \mathcal{H}'(t), \sigma], \qquad [1]$$

where

$$\mathcal{H}_0(t) = -[\omega_{0\mathrm{I}} I_z + \omega_{0\mathrm{S}} S_z + \omega_{\mathrm{r}}(S_x \cos \omega_{\mathrm{S}} t + S_y \sin \omega_{\mathrm{S}} t)],$$
$$\mathcal{H}_J = J\mathbf{I}\cdot\mathbf{S} \qquad [2]$$

with $\omega_{0\mathrm{I}}$ (ω_{I}) and $\omega_{0\mathrm{S}}$ (ω_{S}) as the Larmor frequencies for the I and S spins respectively and ω_{r} as the RF field strength in the vicinity of S-spin resonance in units of radians per second. $\mathcal{H}_1(t)$ includes the quadrupolar relaxation Hamiltonian of spin S, dipolar interaction between spins I and S, and the CSA for spin I,

$$\mathcal{H}'(t) = \mathcal{H}'^{\mathrm{Q}}(t) + \mathcal{H}'^{\mathrm{D}}(t) + \mathcal{H}'^{\mathrm{C}}(t). \qquad [3]$$

Transforming to a doubly rotating frame with

$$\mathsf{R}(t) = \exp(i\omega_{\mathrm{I}} I_z t)\exp(i\omega_{\mathrm{S}} S_z t)$$
$$\boldsymbol{\sigma}^*(t) = \mathsf{R}(t)\boldsymbol{\sigma}(t)\mathsf{R}^{-1}(t) \qquad [4]$$

and using the standard treatment for relaxation (*4*) yields

$$\frac{d\boldsymbol{\sigma}^*}{dt} = -i[\mathcal{H}_0^* + \mathcal{H}_J^*, \boldsymbol{\sigma}^*] - \Gamma(\boldsymbol{\sigma}^* - \boldsymbol{\sigma}_0), \qquad [5]$$

where

$$\mathcal{H}_0^* = -(\Delta\omega_{\mathrm{I}} I_z + \Delta\omega_{\mathrm{S}} S_z + \omega_{\mathrm{r}} S_x),$$
$$\mathcal{H}_J^* = J I_z S_z,$$
$$\Delta\omega_{\mathrm{I}} = \omega_{0\mathrm{I}} - \omega_{\mathrm{I}},\ \Delta\omega_{\mathrm{S}} = \omega_{0\mathrm{S}} - \omega_{\mathrm{S}}, \qquad [6]$$

and Γ is the relaxation super operator (*14*) corresponding to the Hamiltonian $\mathcal{H}_1(t)$. In $\mathcal{H}_J$, only the JI_zS_z term is retained for further calculations. If the quadrupolar relaxation of spin S is strong such that the spin coupling is totally obliterated, $\mathcal{H}_J$ may be written as $J\mathbf{I}\cdot\mathbf{S}(t)$ leading to scalar relaxation of the second kind (*4*). If this is the case, the lineshape calculation is simpler than the general case presented here. The derivation of longitudinal and transverse-relaxation rates of spin I for such a case in the presence of strong RF irradiation of spin S is described briefly in the Appendix.

The six spin-product states $|m_I, m_S\rangle$ of the I–S spin system are

$$|1\rangle = |\tfrac{1}{2}, 1\rangle,\ |2\rangle = |\tfrac{1}{2}, 0\rangle,\ |3\rangle = |\tfrac{1}{2}, -1\rangle,$$

$$|4\rangle = |-\tfrac{1}{2}, 1\rangle,\ |5\rangle = |-\tfrac{1}{2}, 0\rangle, \text{ and } |6\rangle = |-\tfrac{1}{2}, -1\rangle.$$

In the absence of any S-spin decoupling field, the I-spin spectrum is a triplet with frequencies given by

$$\omega^I_{ab} = \Delta\omega_I + Jm_S, \qquad [7]$$

where

$$|a\rangle = |-\tfrac{1}{2}, m_S\rangle \text{ and } |b\rangle = |\tfrac{1}{2}, m_S\rangle.$$

For calculation purposes, it is convenient to rewrite Eq. [5] as $d\boldsymbol{\sigma}^*/dt = \mathsf{A}\boldsymbol{\sigma}^*$, where

$$\mathsf{A}\boldsymbol{\sigma}^* = -i[H_0^* + H_J^*, \boldsymbol{\sigma}^*] - \Gamma(\boldsymbol{\sigma}^* - \boldsymbol{\sigma}_0). \qquad [8]$$

A formal solution of Eq. [8] may be written as

$$\boldsymbol{\sigma}^*(t) = e^{\mathsf{A}t}\boldsymbol{\sigma}^*(0), \qquad [9]$$

where $\boldsymbol{\sigma}^*(0)$ is the density matrix immediately following a $\pi/2$ pulse on the I spin and is given by a unit column vector, and A is a 3×3 matrix. Following the procedure given in Chap. X of Ref. (*4*), the time-domain signal arising from the free-induction decay of the three single-quantum I-spin transitions (I_1, I_2, and I_3) can be represented as

$$G(t) = \mathbf{X}\,\boldsymbol{\sigma}^*(t) = \mathrm{X}e^{\mathsf{A}t}\boldsymbol{\sigma}^*(0), \qquad [10]$$

where $\mathbf{X}$ is a row vector with elements (1, 1, 1) equal to the normalized intensities of the lines in the spectrum in the absence of any relaxation. The spectrum is then given by the Fourier transform of $G(t)$, i.e.,

$$F(\omega) = \mathrm{re}\left[\mathbf{X}\cdot\left\{\int_0^\infty e^{(\mathsf{A}-i\omega\mathsf{E})t}dt\right\}\cdot\boldsymbol{\sigma}^*(0)\right]. \qquad [11]$$

In the above, E is a unit matrix and re stands for the real part. Evaluation of the above integration yields

$$F(\omega) = \mathrm{re}[\mathbf{X}\cdot[\mathsf{A} - i\omega\mathsf{E}]^{-1}\cdot\boldsymbol{\sigma}^*(0)]. \qquad [12]$$

The situation becomes complicated in the presence of an S-spin decoupling field. Six additional multiple-quantum coherences (MQs), two zero-quantum (Z_1, Z_2), two double-quantum (D_1, D_2), one two-spin-flip single-quantum (2s1q), and one two-spin-flip three-quantum (2s3q) coherences will now be coupled to the three single-quantum coherences I_1, I_2, I_3, so that the dimension of Eqs. [9] through [12] becomes 9 instead of the 3 which it is in the absence of irradiation. The elements of $\boldsymbol{\sigma}^*$ corresponding to the nine coherences are given by

$$\begin{aligned}
I_1 &= \langle\tfrac{1}{2}, 1|\boldsymbol{\sigma}^*|-\tfrac{1}{2}, 1\rangle = \langle 1|\boldsymbol{\sigma}^*|4\rangle,\\
I_2 &= \langle\tfrac{1}{2}, 0|\boldsymbol{\sigma}^*|-\tfrac{1}{2}, 0\rangle = \langle 2|\boldsymbol{\sigma}^*|5\rangle,\\
I_3 &= \langle\tfrac{1}{2}, -1|\boldsymbol{\sigma}^*|-\tfrac{1}{2}, -1\rangle = \langle 3|\boldsymbol{\sigma}^*|6\rangle,\\
Z_1 &= \langle\tfrac{1}{2}, 0|\boldsymbol{\sigma}^*|-\tfrac{1}{2}, 1\rangle = \langle 2|\boldsymbol{\sigma}^*|4\rangle,\\
D_1 &= \langle\tfrac{1}{2}, 1|\boldsymbol{\sigma}^*|-\tfrac{1}{2}, 0\rangle = \langle 1|\boldsymbol{\sigma}^*|5\rangle,\\
Z_2 &= \langle\tfrac{1}{2}, -1|\boldsymbol{\sigma}^*|-\tfrac{1}{2}, 0\rangle = \langle 3|\boldsymbol{\sigma}^*|5\rangle,\\
D_2 &= \langle\tfrac{1}{2}, 0|\boldsymbol{\sigma}^*|-\tfrac{1}{2}, -1\rangle = \langle 2|\boldsymbol{\sigma}^*|6\rangle,\\
\text{2s1q} &= \langle\tfrac{1}{2}, -1|\boldsymbol{\sigma}^*|-\tfrac{1}{2}, 1\rangle = \langle 3|\boldsymbol{\sigma}^*|4\rangle,\\
\text{2s3q} &= \langle\tfrac{1}{2}, 1|\boldsymbol{\sigma}^*|-\tfrac{1}{2}, -1\rangle = \langle 1|\boldsymbol{\sigma}^*|6\rangle. \qquad [13]
\end{aligned}$$

The matrix elements of $\Gamma(\boldsymbol{\sigma}^* - \boldsymbol{\sigma}_0)$ appearing in the A matrix (see Eq. [8]) can be defined by the equations

$$\begin{aligned}
\langle\alpha|\Gamma(\boldsymbol{\sigma}^* - \boldsymbol{\sigma}_0)|\alpha'\rangle &= \sum_{\beta\beta'} R_{\alpha\alpha'\beta\beta'}(\boldsymbol{\sigma}^* - \boldsymbol{\sigma}_0)_{\beta\beta'}\\
&\quad - i(\delta\omega_{\alpha\alpha'}\sigma^*_{\alpha\alpha'})_{\alpha\neq\alpha'}, \qquad [14]
\end{aligned}$$

and

$$\begin{aligned}
R_{\alpha\alpha'\beta\beta'} &= \tfrac{1}{2}\{J_{\alpha\beta\alpha'\beta'} + J_{\beta'\alpha'\beta\alpha}\\
&\quad - \delta_{\alpha'\beta'}\sum_\gamma J_{\alpha\gamma\beta\gamma} - \delta_{\alpha\beta}\sum_\gamma J_{\gamma\alpha'\gamma\beta'}\}, \qquad [15]
\end{aligned}$$

with

$$\begin{aligned}
J_{\alpha\beta\alpha'\beta'} &= \int_{-\infty}^{\infty}\langle\langle\alpha|H'(t)|\beta\rangle\\
&\quad \times \langle\alpha'|\mathsf{R}^{-1}(\tau)H'(t-\tau)\mathsf{R}(\tau)|\beta'\rangle^*\rangle_{\mathrm{av}}d\tau, \qquad [16]
\end{aligned}$$

in which $\langle\,\rangle_{\mathrm{av}}$ represents an ensemble average, and $\delta\omega_{\alpha\alpha'}$ represents a dynamic frequency shift defined later in Eq. [21].

For the calculation of $J_{\alpha\beta\alpha'\beta'}$, it is convenient to express the three relaxation Hamiltonians in terms of their irreducible spherical tensor components as

TABLE 1
Lattice Functions F_q and Spin Operators A_q in the Relaxation Hamiltonians

Quadrupolar relaxation	Dipolar relaxation	CSA relaxation
$F_q^{\mathrm{Q}} = \sqrt{\frac{3}{2}}\frac{e^2qQ}{2S(2S-1)}$	$F_q^{\mathrm{D}} = -\sqrt{6}\frac{\gamma_I\gamma_S\hbar}{r_{IS}^3}D_{0q}^{(2)}(\Omega_{\mathrm{D}})$.	$F_q^{\mathrm{C_I}} = \sqrt{\frac{3}{2}}\delta_{zz}$
$[D_{0q}^{(2)}(\Omega_{\mathrm{Q}}) - \sqrt{\frac{1}{6}}\eta_{\mathrm{Q}}D_{+2q}^{(2)}(\Omega_{\mathrm{Q}}) - \sqrt{\frac{1}{6}}\eta_{\mathrm{Q}}D_{-2q}^{(2)}(\Omega_{\mathrm{Q}})]$.	$A_0^{\mathrm{D}} = \frac{1}{\sqrt{6}}(3I_zS_z - \mathbf{I}\cdot\mathbf{S})$	$[D_{0q}^{(2)}(\Omega_{\mathrm{C_I}}) - \sqrt{\frac{1}{6}}\eta_{\mathrm{C_I}}D_{+2q}^{(2)}(\Omega_{\mathrm{C_I}}) - \sqrt{\frac{1}{6}}\eta_{\mathrm{C_I}}D_{-2q}^{(2)}(\Omega_{\mathrm{C_I}})]$.
$A_0^{\mathrm{Q}} = \frac{1}{\sqrt{6}}[3S_z^2 - S(S+1)]$	$A_{\pm1}^{\mathrm{D}} = \mp\frac{1}{2}(I_zS_\pm + I_\pm S_z)$	$A_0^{\mathrm{C_I}} = \frac{2}{\sqrt{6}}\omega_I I_z$.
$A_{\pm1}^{\mathrm{Q}} = \mp\frac{1}{2}(S_zS_\pm + S_\pm S_z)$	$A_{\pm2}^{\mathrm{D}} = \frac{1}{2}I_\pm S_\pm$.	$A_{\pm1}^{\mathrm{C_I}} = \mp\frac{1}{2}\omega_I I_\pm$
$A_{\pm2}^{\mathrm{Q}} = \frac{1}{2}S_\pm^2$.		$A_{\pm2}^{\mathrm{C_I}} = 0$.

Note. See Eq. [17] in the text. The Hamiltonians are expressed in angular frequency units. The expressions are in standard notation. Superscripts Q, D, and C denote the three relaxation mechanisms. e^2qQ is the quadrupolar coupling constant in radians per second. γ_I and γ_S are gyromagnetic ratios of spin I and S and r_{IS} is the distance between them. η_{Q} and $\eta_{\mathrm{C_I}}$ are the asymmetry parameters for quadrupolar and CSA interactions, respectively. δ_{zz} is the largest principal value of the CSA tensor. $D_{q'q}^{(1)}(\Omega)$ are the Wigner rotation matrices. For further details, see Refs. (*20–22*).

$$H'(t) = \sum_{q=-2}^{2}(-1)^q F_q(t)A_{-q}, \qquad [17]$$

where F_q are the lattice functions and A_q are the spin operators such that, $F_q^* = (-1)^q F_{-q}$ and $A_q^\dagger = (-1)^q A_{-q}$. The various F_q and A_q for the three relaxation mechanisms (*21*, *22*) are given in Table 1. The calculation of the spectral densities may now proceed along the lines described, for example, in Ref. (*17*). Assuming an isotropic motion described by a correlation time τ_c leads to Lorentzian spectral densities through

$$\langle F_q(t)F_{q'}^*(t-\tau)\rangle_{\mathrm{av}} = \delta_{qq'}\langle|F_q|^2\rangle_{\mathrm{av}}\exp(-|\tau|/\tau_c),$$

and

$$\tfrac{1}{2}\int_{-\infty}^{\infty}\exp(i\omega_q\tau)\exp(-|\tau|/\tau_c)d\tau = \frac{\tau_c}{1+\omega_q^2\tau_c^2} = J(\omega_q). \qquad [18]$$

The $J_{\alpha\beta\alpha'\beta'}$ in Eq. [16] may be expressed as

$$\begin{aligned}\tfrac{1}{2}J_{\alpha\beta\alpha'\beta'} = &\sum_{q=-2}^{2}J(\omega_q^{\mathrm{D}})\langle|F_q^{\mathrm{D}}|^2\rangle_{\mathrm{av}}\langle\alpha|A_{-q}^{\mathrm{D}}|\beta\rangle\langle\alpha'|A_{-q}^{\mathrm{D}}|\beta'\rangle^* \\ &+\sum_{q=-2}^{2}J(\omega_q^{\mathrm{Q}})\langle|F_q^{\mathrm{Q}}|^2\rangle_{\mathrm{av}}\langle\alpha|A_{-q}^{\mathrm{Q}}|\beta\rangle \\ &\times\langle\alpha'|A_{-q}^{\mathrm{Q}}|\beta'\rangle^* \\ &+\sum_{q=-2}^{2}J(\omega_q^{\mathrm{C_I}})\langle|F_q^{\mathrm{C_I}}|^2\rangle_{\mathrm{av}}\langle\alpha|A_{-q}^{\mathrm{C_I}}|\beta\rangle \\ &\times\langle\alpha'|A_{-q}^{\mathrm{C_I}}|\beta'\rangle^* \\ &+\sum_{q=-2}^{2}J(\omega_q^{\mathrm{Q}})\langle|F_q^{\mathrm{D}}F_q^{\mathrm{Q}*}|\rangle_{\mathrm{av}}\langle\alpha|A_{-q}^{\mathrm{D}}|\beta\rangle \\ &\times\langle\alpha'|A_{-q}^{\mathrm{Q}}|\beta'\rangle^* \\ &+\sum_{q=-2}^{2}J(\omega_q^{\mathrm{D}})\langle|F_q^{\mathrm{Q}}F_q^{\mathrm{D}*}|\rangle_{\mathrm{av}}\langle\alpha|A_{-q}^{\mathrm{Q}}|\beta\rangle \\ &\times\langle\alpha'|A_{-q}^{\mathrm{D}}|\beta'\rangle^* \\ &+\sum_{q=-2}^{2}J(\omega_q^{\mathrm{C_I}})\langle|F_q^{\mathrm{D}}F_q^{\mathrm{C_I}*}|\rangle_{\mathrm{av}}\langle\alpha|A_{-q}^{\mathrm{D}}|\beta\rangle \\ &\times\langle\alpha'|A_{-q}^{\mathrm{C_I}}|\beta'\rangle^* \\ &+\sum_{q=-2}^{2}J(\omega_q^{\mathrm{D}})\langle|F_q^{\mathrm{C_I}}F_q^{\mathrm{D}*}|\rangle_{\mathrm{av}}\langle\alpha|A_{-q}^{\mathrm{C_I}}|\beta\rangle \\ &\times\langle\alpha'|A_{-q}^{\mathrm{D}}|\beta'\rangle^*. \end{aligned} \qquad [19]$$

In Eq. [19], the first three terms are the auto-correlation relaxation rates, the fourth and fifth terms are the cross correlations between dipolar and quadrupolar relaxation mechanisms, and the last two terms are the cross correlations between the dipolar and CSA relaxation mechanisms. Using the orthogonality of the Wigner rotation matrices, the various averages in Eq. [19] are given by

$$\langle |F_q^{\mathrm{D}}|^2\rangle_{\mathrm{av}} = \frac{6}{5}\frac{\gamma_{\mathrm{I}}^2\gamma_{\mathrm{S}}^2\hbar^2}{r_{\mathrm{IS}}^6},$$

$$\langle |F_q^{\mathrm{Q}}|^2\rangle_{\mathrm{av}} = \frac{3}{40}\frac{(e^2qQ)^2}{[S(2S-1)]^2}\left(1+\frac{\eta_{\mathrm{Q}}^2}{3}\right),$$

$$\langle |F_{q^{\mathrm{I}}}^{\mathrm{C_I}}|^2\rangle_{\mathrm{av}} = \frac{3}{10}\delta_{zz}^2\left(1+\frac{\eta_{\mathrm{C_I}}^2}{3}\right),$$

$$\begin{aligned}\langle |F_q^{\mathrm{D}}F_q^{\mathrm{Q}*}|\rangle_{\mathrm{av}} &= \langle |F_q^{\mathrm{Q}}F_q^{\mathrm{D}*}|\rangle_{\mathrm{av}}\\ &= -\frac{3}{10}\frac{\gamma_{\mathrm{I}}\gamma_{\mathrm{S}}\hbar}{r_{\mathrm{IS}}^3}\frac{(e^2qQ)}{2S(2S-1)}\\ &\quad\times[(3\cos^2\theta_{\mathrm{Q-D}}-1)\\ &\quad-\eta_{\mathrm{Q}}\sin^2\theta_{\mathrm{Q-D}}\cos 2\phi_{\mathrm{Q-D}}],\end{aligned}$$

and

$$\begin{aligned}\langle |F_q^{\mathrm{D}}F_q^{\mathrm{C_I}*}|\rangle_{\mathrm{av}} &= \langle |F_{q^{\mathrm{I}}}^{\mathrm{C_I}}F_q^{\mathrm{D}*}|\rangle_{\mathrm{av}}\\ &= -\frac{3}{10}\frac{\gamma_{\mathrm{I}}\gamma_{\mathrm{S}}\hbar}{r_{\mathrm{IS}}^3}\delta_{zz}[(3\cos^2\theta_{\mathrm{C_I-D}}-1)\\ &\quad-\eta_{\mathrm{C_I}}\sin^2\theta_{\mathrm{C_I-D}}\cos 2\phi_{\mathrm{C_I-D}}],\end{aligned}\qquad[20]$$

where $\theta_{\mathrm{Q-D}}/\theta_{\mathrm{C_I-D}}$ and $\phi_{\mathrm{Q-D}}/\phi_{\mathrm{C_I-D}}$ are respectively the polar and azimuthal angles of the dipolar vector in the principal axis system of the quadrupolar tensor/CSA tensor.

The dynamic shifts represented by $\delta\omega_{\alpha\alpha'}$ are given by

$$\begin{aligned}\delta\omega_{\alpha\alpha'} &= L_{\alpha\alpha'\alpha\alpha'}\\ &= K_{\alpha\alpha\alpha'\alpha'} + K_{\alpha'\alpha'\alpha\alpha} - \sum_{\gamma}K_{\alpha\gamma\alpha\gamma} - \sum_{\gamma}K_{\gamma\alpha'\gamma\alpha'},\end{aligned}\quad[21a]$$

where

$$K_{\alpha\beta\alpha'\beta'} = \mathrm{Im}\left(\int_0^\infty \langle\langle\alpha|H'(t)|\beta\rangle \times\langle\alpha'|\mathsf{R}^{-1}(\tau)H'(t-\tau)\mathsf{R}(\tau)|\beta'\rangle^*\rangle_{\mathrm{av}}d\tau\right),\qquad[21]$$

where Im stands for the imaginary part. These terms add to the first term in Eq. [8], thereby modifying the frequency of the transition $\alpha\rightarrow\alpha'$. Such dynamic-shift terms arise for all spectral densities at nonzero frequencies in Eq. [21]. However, in the absence of spin–spin coupling, the dynamic shifts change $\omega_{0\mathrm{I}}$ and $\omega_{0\mathrm{S}}$, i.e., effectively alter the chemical shifts which are not readily detected, although they are observable in specially designed experiments. However, in the presence of spin–spin coupling, if the dynamic shifts are different for different multiplet resonances, these effects are seen as a change in spin–spin multiplet patterns (*19, 20*). We consider only such shifts in the present calculations. For the $I=\frac{1}{2}, S=1$ coupled spin system, dynamic-shifts differential with respect to the spin–spin multiplet arise from the imaginary part of the quadrupolar–dipolar cross-correlation term of the longitudinal relaxation of spin S and from the CSA–dipolar cross-correlation term of the longitudinal relaxation of spin I.

The *A* matrix is given on the following page. The relaxation rates $R_{\alpha\alpha'\beta\beta'}$ and the dynamic shifts $\delta\omega_{\alpha\alpha'}$ appearing in A are give in Table 2 and Table 3, respectively. The various spectral density terms such as $J^{\mathrm{Q}}(\omega)$, $J^{\mathrm{D}}(\omega)$ (see Table 2) for the case of $I=\frac{1}{2}$ and $S=1$ are given by

$$J^{\mathrm{Q}}(\omega) = \frac{3}{160}(e^2qQ)^2\left(1+\frac{\eta_{\mathrm{Q}}^2}{3}\right)\frac{\tau_{\mathrm{c}}}{1+\omega^2\tau_{\mathrm{c}}^2},$$

$$J^{\mathrm{D}}(\omega) = \frac{3}{10}\left(\frac{\gamma_{\mathrm{I}}^2\gamma_{\mathrm{S}}^2\hbar^2}{r_{\mathrm{IS}}^6}\right)\frac{\tau_{\mathrm{c}}}{1+\omega^2\tau_{\mathrm{c}}^2},$$

$$J^{\mathrm{C_I}}(\omega) = \frac{3}{10}\omega_{\mathrm{I}}^2\delta_{zz}^2\left(1+\frac{\eta_{\mathrm{C_I}}^2}{3}\right)\frac{\tau_{\mathrm{c}}}{1+\omega^2\tau_{\mathrm{c}}^2},$$

$$\begin{aligned}J^{\mathrm{Q-D}}(\omega) &= \frac{3}{80}\frac{\gamma_{\mathrm{I}}\gamma_{\mathrm{S}}\hbar}{r_{\mathrm{IS}}^3}(e^2qQ)[(3\cos^2\theta_{\mathrm{Q-D}}-1)\\ &\quad-\eta_{\mathrm{Q}}\sin^2\theta_{\mathrm{Q-D}}\cos 2\phi_{\mathrm{Q-D}}]\frac{\tau_{\mathrm{c}}}{1+\omega^2\tau_{\mathrm{c}}^2},\end{aligned}$$

and

$$\begin{aligned}J^{\mathrm{C_I-D}}(\omega) &= \frac{3}{10}\frac{\gamma_{\mathrm{I}}\gamma_{\mathrm{S}}\hbar}{r_{\mathrm{IS}}^3}\omega_{\mathrm{I}}\delta_{zz}[(3\cos^2\theta_{\mathrm{C_I-D}}-1)\\ &\quad-\eta_{\mathrm{C_I}}\sin^2\theta_{\mathrm{C_I-D}}\cos 2\phi_{\mathrm{C_I-D}}]\\ &\quad\times\frac{\tau_{\mathrm{c}}}{1+\omega^2\tau_{\mathrm{c}}^2}.\end{aligned}\qquad[23]$$

The imaginary part of the spectral densities which determine $\delta\omega_{\alpha\alpha'}$ in Table 3 are given by

$$L^{\mathrm{Q-D}}(\omega) = \omega\tau_{\mathrm{c}}J^{\mathrm{Q-D}}(\omega),$$

and

$$L^{\mathrm{C_I-D}}(\omega) = \omega\tau_{\mathrm{c}}J^{\mathrm{C_I-D}}(\omega).\qquad[24]$$

SIMULATIONS

Lineshapes of a ^{13}C nucleus (I) coupled to a deuterium nucleus (S) which is subjected to a decoupling field were

$$
\mathsf{A} = \begin{bmatrix}
-i(\Delta\omega_{\mathrm{I}} + J + \delta\omega_{14}) + R_{1414} & R_{1425} & R_{1436} & \frac{-i\omega_{\mathrm{r}}}{\sqrt{2}} & \frac{i\omega_{\mathrm{r}}}{\sqrt{2}} & 0 & 0 & 0 & 0 \\
R_{2514} & -i(\Delta\omega_{\mathrm{I}} + \delta\omega_{25}) + R_{2525} & R_{2536} & \frac{i\omega_{\mathrm{r}}}{\sqrt{2}} & \frac{-i\omega_{\mathrm{r}}}{\sqrt{2}} & \frac{-i\omega_{\mathrm{r}}}{\sqrt{2}} & \frac{i\omega_{\mathrm{r}}}{\sqrt{2}} & 0 & 0 \\
R_{3614} & R_{3625} & -i(\Delta\omega_{\mathrm{I}} - J + \delta\omega_{36}) + R_{3636} & 0 & 0 & \frac{i\omega_{\mathrm{r}}}{\sqrt{2}} & \frac{-i\omega_{\mathrm{r}}}{\sqrt{2}} & 0 & 0 \\
\frac{-i\omega_{\mathrm{r}}}{\sqrt{2}} & \frac{i\omega_{\mathrm{r}}}{\sqrt{2}} & 0 & -i(\Delta\omega_{\mathrm{I}} - \Delta\omega_{\mathrm{S}} + \frac{J}{2} + \delta\omega_{24}) + R_{2424} & 0 & 0 & 0 & \frac{-i\omega_{\mathrm{r}}}{\sqrt{2}} & 0 \\
\frac{i\omega_{\mathrm{r}}}{\sqrt{2}} & \frac{-i\omega_{\mathrm{r}}}{\sqrt{2}} & 0 & 0 & -i(\Delta\omega_{\mathrm{I}} + \Delta\omega_{\mathrm{S}} + \frac{J}{2} + \delta\omega_{15}) + R_{1515} & 0 & 0 & 0 & \frac{i\omega_{\mathrm{r}}}{\sqrt{2}} \\
0 & \frac{-i\omega_{\mathrm{r}}}{\sqrt{2}} & \frac{i\omega_{\mathrm{r}}}{\sqrt{2}} & 0 & 0 & -i(\Delta\omega_{\mathrm{I}} - \Delta\omega_{\mathrm{S}} - \frac{J}{2} + \delta\omega_{35}) + R_{3535} & 0 & \frac{i\omega_{\mathrm{r}}}{\sqrt{2}} & 0 \\
0 & \frac{i\omega_{\mathrm{r}}}{\sqrt{2}} & \frac{-i\omega_{\mathrm{r}}}{\sqrt{2}} & 0 & 0 & 0 & -i(\Delta\omega_{\mathrm{I}} + \Delta\omega_{\mathrm{S}} + \frac{J}{2} + \delta\omega_{26}) + R_{2626} & 0 & \frac{-i\omega_{\mathrm{r}}}{\sqrt{2}} \\
0 & 0 & 0 & \frac{-i\omega_{\mathrm{r}}}{\sqrt{2}} & 0 & \frac{i\omega_{\mathrm{r}}}{\sqrt{2}} & 0 & -i(\Delta\omega_{\mathrm{I}} - 2\Delta\omega_{\mathrm{S}} + \delta\omega_{34}) + R_{3434} & 0 \\
0 & 0 & 0 & 0 & \frac{i\omega_{\mathrm{r}}}{\sqrt{2}} & 0 & \frac{-i\omega_{\mathrm{r}}}{\sqrt{2}} & 0 & -i(\Delta\omega_{\mathrm{I}} + 2\Delta\omega_{\mathrm{S}} + \delta\omega_{16}) + R_{1616}
\end{bmatrix}
$$

[22]

TABLE 2
The Redfield Relaxation Elements Appearing in the A Matrix

$$R_{1414/3636} = -[4J^{Q}(\omega_S) + 8J^{Q}(2\omega_S) + \tfrac{8}{3}J^{D}(0) + \tfrac{1}{3}J^{D}(\omega_I - \omega_S) + 2J^{D}(\omega_I) + J^{D}(\omega_S) + 2J^{D}(\omega_I + \omega_S) + \tfrac{2}{3}J^{C_I}(0) + \tfrac{1}{2}J^{C_I}(\omega_I)] \pm [\tfrac{4}{3}J^{C_I-D}(0) + J^{C_I-D}(\omega_I)]$$

$$R_{2525} = -[8J^{Q}(\omega_S) + \tfrac{2}{3}J^{D}(\omega_I - \omega_S) + 2J^{D}(\omega_S) + 4J^{D}(\omega_I + \omega_S) + \tfrac{2}{3}J^{C_I}(0) + \tfrac{1}{2}J^{C_I}(\omega_I)]$$

$$R_{1425} = R_{2514} = 4J^{Q}(\omega_S) - J^{D}(\omega_S)$$

$$R_{1436} = R_{3614} = 8J^{Q}(2\omega_S)$$

$$R_{2424/3535} = -[6J^{Q}(0) + 6J^{Q}(\omega_S) + 4J^{Q}(2\omega_S) + \tfrac{2}{3}J^{D}(0) + \tfrac{2}{3}J^{D}(\omega_I - \omega_S) + J^{D}(\omega_I) + \tfrac{3}{2}J^{D}(\omega_S) + 2J^{D}(\omega_I + \omega_S) + \tfrac{2}{3}J^{C_I}(0) + \tfrac{1}{2}J^{C_I}(\omega_I)] - [4J^{Q-D}(0) + 2J^{Q-D}(\omega_S)] \pm [\tfrac{1}{3}J^{C_I-D}(0) + \tfrac{1}{2}J^{C_I-D}(\omega_I)]$$

$$R_{1515/2626} = -[6J^{Q}(0) + 6J^{Q}(\omega_S) + 4J^{Q}(2\omega_S) + \tfrac{2}{3}J^{D}(0) + \tfrac{1}{3}J^{D}(\omega_I - \omega_S) + J^{D}(\omega_I) + \tfrac{3}{2}J^{D}(\omega_S) + 4J^{D}(\omega_I + \omega_S) + \tfrac{2}{3}J^{C_I}(0) + \tfrac{1}{2}J^{C_I}(\omega_I)] - [4J^{Q-D}(0) + 2J^{Q-D}(\omega_S)] \pm [\tfrac{1}{3}J^{C_I-D}(0) + \tfrac{1}{2}J^{C_I-D}(\omega_I)]$$

$$R_{3434} = -[4J^{Q}(\omega_S) + 8J^{Q}(2\omega_S) + \tfrac{2}{3}J^{D}(\omega_I - \omega_S) + 2J^{D}(\omega_I) + J^{D}(\omega_S)] + 4J^{Q-D}(\omega_S)$$

$$R_{1616} = -[4J^{Q}(\omega_S) + 8J^{Q}(2\omega_S) + 4J^{D}(\omega_I + \omega_S) + 2J^{D}(\omega_I) + J^{D}(\omega_S)] + 4J^{Q-D}(\omega_S)$$

Note. The various spectral density terms such as $J^{Q}(\omega)$, $J^{D}(\omega)$, etc., are defined in Eq. [23] (see text).

simulated on the basis of Eq. [12] with the A matrix given in Eq. [14]. The parameters common to all the simulations were $J/2\pi(^{13}C-^{2}H) = 22$ Hz, $\tau_c = 20$ ns, $e^2qQ = 1.1 \times 10^6$ s^{-1}, and $\gamma_I\gamma_S\hbar/r_{IS}^3 = 22 \times 10^3$ s^{-1}. In Figs. 3 and 4, the CSA of the spin I was also included with $\delta_{zz} = 100$ ppm. For simplicity, the asymmetry parameters η_Q and η_{C_I} and polar angles θ_{Q-D} and θ_{C_I-D} were set equal to zero in all the simulations. In Figs. 1–3, the proton Larmor frequency was chosen to be 600 MHz, and, at this frequency, the value of the longitudinal relaxation time of the quadrupolar nucleus, $T_{1Q} = [4J^{Q}(\omega) + 16J^{Q}(2\omega)]^{-1}$ (*4*), is about 43 ms. In Fig. 4, the proton Larmor frequency was 190 MHz and the computed T_{1Q} is 4.5 ms. It has been shown that, in the extreme narrowing limit and in the absence of any decoupling field, as the parameter $(5T_{1Q}J)^2$ is varied from 1000 to 1 the I-spin spectrum changes from a fully resolved triplet to a narrow singlet and is a broad singlet when $(5T_{1Q}J)^2 = 10$ (*3*). The product $(5T_{1Q}J)^2$ is a useful parameter to predict the nature of the multiplet structures even when the extreme narrowing limit is not valid, as in the present simulations in which $\omega_{0S}\tau_c > 1$. Thus, in the absence of any ^{2}H decoupling field, in Figs. 1–3, wherein the value of $(5T_{1Q}J)^2 \approx 880$, the multiplet structure is expected to be a triplet, and, in Fig. 4, the multiplet structure is a collapsed singlet since $(5T_{1Q}J)^2 \approx 10$.

TABLE 3
Dynamic Shifts Appearing in the *A* Matrix

$$\delta\omega_{14} = -4L^{Q-D}(\omega_S) + L^{C_I-D}(\omega_I)$$
$$\delta\omega_{25} = 8L^{Q-D}(\omega_S)$$
$$\delta\omega_{36} = -4L^{Q-D}(\omega_S) - L^{C_I-D}(\omega_I)$$
$$\delta\omega_{24} = \delta\omega_{15} = 2L^{Q-D}(\omega_S) + \tfrac{1}{2}L^{C_I-D}(\omega_I)$$
$$\delta\omega_{35} = \delta\omega_{26} = 2L^{Q-D}(\omega_S) - \tfrac{1}{2}L^{C_I-D}(\omega_I)$$
$$\delta\omega_{34} = \delta\omega_{16} = -4L^{Q-D}(\omega_S)$$

Note. The terms $L^{Q-D}(\omega_S)$ and $L^{C_I-D}(\omega_I)$ are defined in Eq. [24] (and Eq. [23]) (see text).

In Fig. 1, only the quadrupolar and dipolar relaxation mechanisms were considered. Although the cross correlations of the two relaxation mechanisms were included in the relaxation rates, and these appear only for the multiple quantum coherences, the dynamic shifts were omitted in order to contrast with Fig. 2 in which they are included. The expected triplet structure is seen in the absence of S-decoupling (Fig. 1a). In Figs. 1b–1h, the simulated lineshapes with RF field strengths $\nu_r = \omega_r/2\pi$ of 11, 22, 50, 100, 150, 500, and 1000 Hz, respectively, applied to ^{2}H nucleus on resonance are presented. In the simulation of Fig. 1b ($\nu_r = 11$ Hz), the ratio $\omega_r/J = 0.5$ and the multiplet structure is little affected as the decoupling field strength was insufficient and the situation remains about the same even for $\omega_r/J = 1$ (Fig. 1c). When the ratio was increased to about 2, as in Fig. 1d ($\nu_r = 50$ Hz), the central line was sharpened. The intensities of the outer lines in the multiplet structure were also reduced. For $\omega_r/J \approx 5$ ($\nu_r = 100$ Hz) (Fig. 1e), the multiplet structure is only partially collapsed and the outer lines were broadened and merged with the base of the central line. However, at about $\omega_r/J \approx 7$ ($\nu_r = 150$ Hz), the collapse of the multiplet structure is complete and a broad singlet appears as the spectrum (Fig. 1f). A further increase of ν_r to a value of 500 Hz sharpened the singlet (Fig. 1g). A subsequent increase of ν_r to a value of 1000 Hz (Fig. 1h) further narrowed the line and the decoupling was more or less complete. There was no further change in

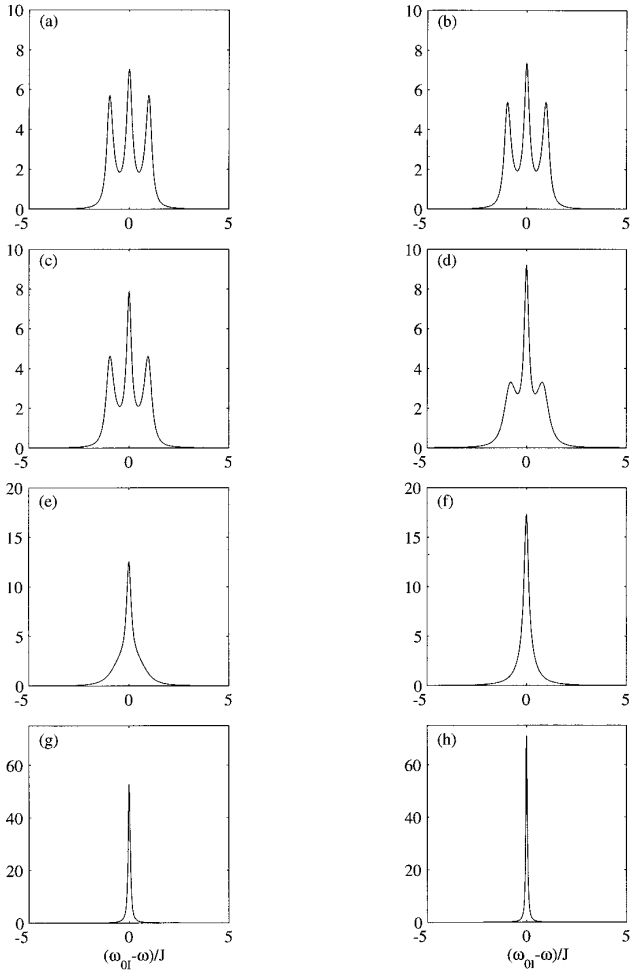

FIG. 1. Simulated ^{13}C spectra of a $^{13}C-^{2}H$ spin system. The spectra were plotted as a function $(\omega_{0I} - \omega/J)$. The parameters used in the simulation are $J/2\pi(^{13}C-^{2}H) = 22$ Hz, $\tau_c = 20$ ns, $e^2qQ = 1.1 \times 10^6$ s^{-1}, $\eta_Q = 0$, $\gamma_I\gamma_S\hbar/r_{IS}^3 = 22 \times 10^3$ s^{-1}, and the proton Larmor frequency was set at 600 MHz. The irradiation amplitudes $\nu_r = \omega_r/2\pi$ in (a) 0, (b) 11, (c) 22, (d) 50, (e) 100, (f) 150, (g) 500, and (h) 1000 Hz. Dynamic shifts were not included in these spectra. Note that the vertical scales are not the same in all the figures.

the lineshape for any more increase in ν_r (data not shown). It can be clearly seen from these simulations that the complete decoupling takes place in two stages as the decoupling field is increased. In the first stage, a collapse of the multiplet structure occurs (Fig. 1f), and, in the second stage, the residual linewidth coming from the scalar relaxation is removed (Figs. 1g and 1h).

In Fig. 2, the ^{13}C lineshapes correspond to a case wherein the dynamic shifts arising from the cross correlations of the quadrupolar and dipolar relaxation mechanisms were also included. The dynamic shifts arise for all the single- and multiple-quantum coherences. In Figs. 2b–2h, ν_r was varied from 11 to 1000 Hz as in Fig. 1. The dynamic shifts as well as the relaxation rates arising from the cross correlations are differential in the multiplets. The shift is the same for the two outer lines and is larger by a factor of two for the central line (see Table 3). The irradiating RF field reduces the dynamic shift and it causes the collapse of the spin multiplet. The magnitudes of the various parameters used in the simulations determine the extent of reduction in the two kinds of splitting. Thus, in Fig. 2f, at the end of the first stage of decoupling when the collapse of the multiplet structure from spin–spin coupling is complete, a small residual dynamic shift of the central resonance persists. However, for a ν_r of 1000 Hz (Fig. 2h), all the effects, viz., decoupling, vanishing of dynamic shifts, and line narrowing are complete, similar to that in Fig. 1h.

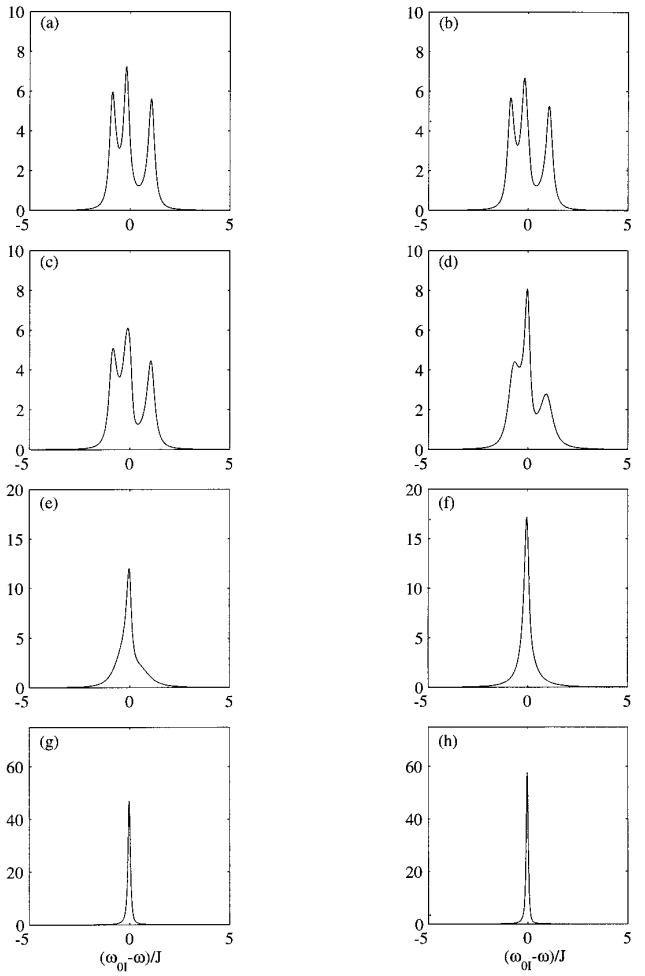

FIG. 2. Simulated ^{13}C spectra of a $^{13}C-^{2}H$ spin system with the same parameters as described in the legend to Fig. 1, and with the dynamic shifts arising from the quadrupole–dipole cross correlation included. The ^{2}H irradiation RF field amplitudes in (a)–(h) are the same as described in the legend to Fig. 1. Note that the vertical scales are not the same in all the figures.

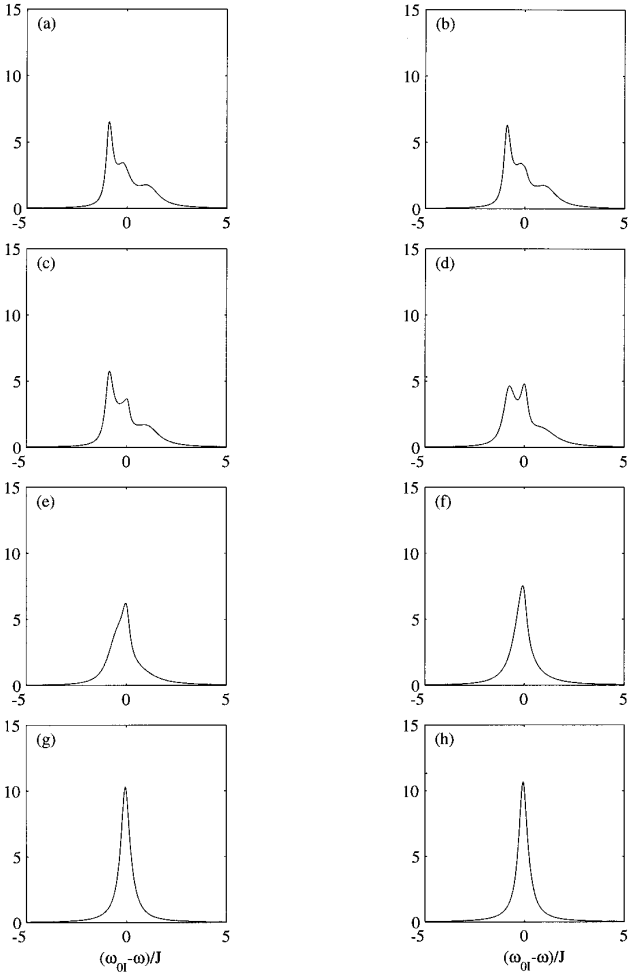

FIG. 3. Simulated ^{13}C spectra of a $^{13}C-^{2}H$ spin system with CSA of spin I ($\delta_{zz} = 100$ ppm, $\eta_{C_I} = 0$) included along with the other interactions in Figs. 1 and 2. Dynamic shifts arising from cross correlations between quadrupolar and dipolar interaction as well as CSA and dipolar interactions are included. The ^{2}H irradiation RF field amplitudes in (a)–(h), and all other parameters are same as described in the legend to Fig. 1.

In Fig. 3, the relaxation arising from chemical-shift anisotropy of spin I is also considered. Dynamic shifts arising from both the cross correlations between quadrupolar and dipolar and that between CSA and dipolar interactions were included. (The S-spin chemical-shift anisotropy was not considered as it is very small for a nucleus such as deuterium). The cross correlation of CSA and dipolar interactions differentially affect the relaxation rates of the outer two lines of the three single-quantum coherences of spin I. The differential effect leads to the appearance of a narrower line on the low-frequency side and a broader line on the high-frequency side (Fig. 3a). The central line is unaffected by this cross correlation both in its relaxation rate and dynamic shift. In Figs. 3b–3h, ν_r was varied between 11 and 1000 Hz and the behavior of the decoupling process is essentially the same as in the previous cases.

A totally different situation is obtained in the simulations shown in Fig. 4, where the proton Larmor frequency was changed to 190 MHz. At this frequency, the T_{1Q} values correspond to 4.5 ms and the parameter $(5T_{1Q}J)^2 \approx 10$. A broad singlet is seen as expected (Fig. 4a); however, the singlet is shifted from the center by the dynamic shifts arising from both cross correlations discussed above. The shift is noticeable since, in the long correlation limit, the linewidths (R_{1414} and R_{3636}) of the outer two lines get contributions from the dominant spectral density at zero frequency from the mutual dipolar relaxation [$J^{D}(0)$] and are very broad compared to the sharp central line (R_{2525}) that is unaffected by the same spectral density (see Table 2]. Thus, although

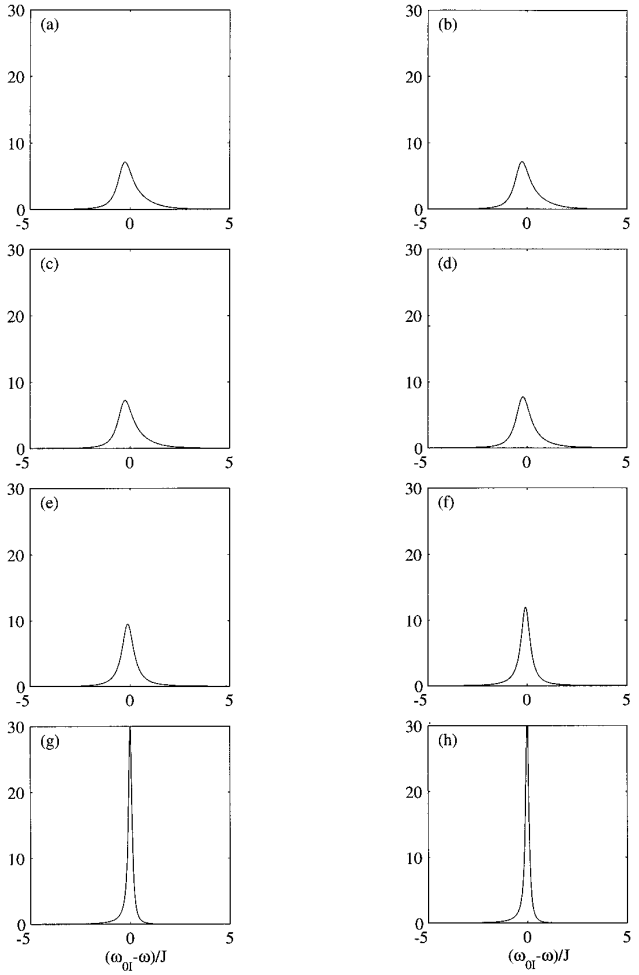

FIG. 4. Simulated ^{13}C spectra of a $^{13}C-^{2}H$ spin system with all the interactions and the parameters used and described in the legend to Fig. 3 except that the proton Larmor frequency was set at 190 MHz and the irradiation amplitudes are $\nu_r = \omega_r/2\pi$ in (a) 0, (b) 11, (c) 22, (d) 50, (e) 100, (f) 150, (g) 1000, and (h) 5000 Hz.

there is a collapse of the multiplet, the dynamic shifts which are differential on the multiplets do not vanish due to the differential linewidths on the three overlapping multiplets. Again, ν_r is varied from 11 to 5000 Hz (Figs. 4b–4h) and as it approaches about 150 Hz (Fig. 4f), the singlet appears at the center. In Fig. 4g ν_r was 1000 Hz and the sharpening of the singlet is complete, and a further increase of ν_r to a value of 5000 Hz (Fig. 4h) did not narrow the line any further.

CONCLUSION

The lineshape analysis presented above illustrates the dependence of the I-spin spectrum on various parameters such as the S-spin quadrupolar longitudinal relaxation time, the scalar coupling between spins I and S, and the strength of the decoupling RF field at the S-spin resonance. When the product $(5T_{1Q}J)^2$ is about 900, as in the simulation of Figs. 1–3, the I-spin spectrum is a triplet in the absence of decoupling. For a given T_{1Q}, the primary condition for complete decoupling is $\omega_r J^{-1} \gg 1$ (and for that decoupling field strength the condition $\omega_r T_{1Q} \gg 1$ will also be satisfied), and the resulting I-spin spectrum is a narrow singlet.

On the other hand, when the product $(5T_{1Q}J)^2$ is about 10, as in the simulation of Fig. 4, the I-spin multiplet structure is collapsed even in the absence of any decoupling field and the J coupling is rendered time dependent, leading to scalar relaxation of the second kind (*4*). The primary contribution to the linewidth due to scalar relaxation comes from the spectral density at zero frequency in the absence of irradiation (see Appendix). The effect of irradiation is to change this frequency from zero to ω_r (Eq. [A8] in the Appendix). By increasing the irradiation strength, ω_r increases, and the linewidth contribution diminishes to a vanishingly small value. Therefore, the condition to suppress this relaxation pathway by irradiation is $\omega_r^2 T_{1Q}^2 \gg 1$ (see Appendix). Thus, as may be seen from Fig. 4g, with $\omega_r T_{1Q} \approx 28$ for $\omega_r/2\pi =$ 1000 Hz and $T_{1Q} = 4.5$ ms, the line narrowing is almost complete. This result is at variance with that reported in an earlier publication by Browne *et al.* (*23*) in which an order of magnitude larger irradiation strength was estimated to reduce such relaxation effects and obtain line narrowing. This incorrect estimate was based on an erroneous equation for the T_2 of spin I. In their paper (*23*), the condition for line narrowing appears as $\omega_r^2 T_{2Q} T_{1Q} \gg 1$ instead of the correct $\omega_r^2 T_{1Q}^2 \gg 1$ as given in Eq. [A8]. It is not clear how these authors have arrived at the term $\omega_r^2 T_{2Q} T_{1Q}$, which appears to be a saturation factor, in the expression for spectral densities for relaxation through scalar coupling. Since, for macromolecules, T_{2Q} is generally smaller than T_{1Q} (at least by a factor of 10), larger RF field strengths were estimated than are actually needed. The reduction in decoupling power is useful from an experimental point of view. It reduces RF heating effects, and, furthermore, when the quadrupolar spin is deuterium, the minimization of RF irradiation reduces interference with the field-frequency lock which usually uses the deuterium signal.

APPENDIX

As described in Abragam's book (*4*), if the I-spin spectrum is a singlet due to rapid relaxation of spin S, the scalar coupling of the two-spin system I and S with $I = \frac{1}{2}$ and $S = 1$ may be considered as a random Hamiltonian in the manner

$$H_1(t) = J\mathbf{I}\cdot\mathbf{S}(t) = \sum_{q=-1}^{1} (-1)^q F_q(t) A_{-q}, \qquad [A1]$$

with

$$A_0 = I_z;\ A_{\pm 1} = \mp\frac{1}{\sqrt{2}} I_{\pm};\ \text{and } F_0 = JS_z;\ F_{\pm 1} = \mp\frac{1}{\sqrt{2}} JS_{\pm}$$

and

$$\overline{S_z(0)S_z(\tau)} = \frac{S(S+1)}{3}\exp(-\tau/T_{1Q}),$$

$$\overline{S_x(0)S_x(\tau)} = \overline{S_y(0)S_y(\tau)} = \frac{S(S+1)}{3}\exp(-\tau/T_{2Q}), \qquad [A2]$$

where the bars over the operators represent time averages due to the rapid relaxation of spin S. Time averages of cross products between different operators vanish.

The equation of motion for the macroscopic observable corresponding to the operator Q in the rotating frame (Eq. [3]) is given as

$$\frac{d\langle Q\rangle}{dt} = -i\langle[\omega_r S_x, Q]\rangle - \left\langle \int_0^\infty d\tau\, \overline{[\exp(-i\omega_r S_x\tau) H_1^*(t-\tau)\exp(i\omega_r S_x\tau), [H_1^*(t), Q]]} \right\rangle, \qquad [A3]$$

where $\langle\ \rangle$ implies taking a trace after multiplying with the density matrix of spin I. The effect of RF on spin S appears in Eq. [A2] in the first term of the right-hand side which is a free precession term, and also as a transformation propagator for the second term in the commutator within the integral. The above equation is the same as that derived for the viscous liquid case in the presence of an RF field (*4*, Chap. XII). In the doubly rotating frame (Eq. 3), the random Hamiltonian is given by $H_1^*(t) = \mathsf{R}(t)H_1(t)\mathsf{R}^{-1}(t)$ with

$$A_0^* = I_z;\ A_1^* = -\frac{1}{\sqrt{2}} I_+ \exp(i\omega_1 t);$$

$$A_{-1}^* = \frac{1}{\sqrt{2}} I_- \exp(-i\omega_1 t),$$

and

$$F_0^* = JS_z;\ F_1^* = -\frac{1}{\sqrt{2}} JS_+ \exp(-i\omega_S t);$$

$$F_{-1}^* = \frac{1}{\sqrt{2}} JS_- \exp(i\omega_S t). \qquad [A4]$$

It remains to compute $\mathsf{T}^{-1}(\tau)H_1^*(t-\tau)\mathsf{T}(\tau)$, where $\mathsf{T}(\tau) = \exp(i\omega_r S_x \tau)$. Since $[T, A_q] = 0$, only the F_q are modified:

$$F_0^* \xrightarrow{\mathsf{T}^{-1}(\tau)} \frac{J}{2}[\exp(i\omega_r\tau)(S_z + iS_y) + \exp(-i\omega_r\tau)(S_z - iS_y),$$

$$F_1^* \xrightarrow{\mathsf{T}^{-1}(\tau)} -\frac{J}{\sqrt{2}}\exp[-i\omega_S(t-\tau)] \times \left[S_x + \frac{1}{2}\{\exp(i\omega_r\tau)(S_z + iS_y) - \exp(-i\omega_r\tau)(S_z - iS_y)\}\right],$$

$$F_{-1}^* \xrightarrow{\mathsf{T}^{-1}(\tau)} \frac{J}{\sqrt{2}}\exp[i\omega_S(t-\tau)] \times \left[S_x - \frac{1}{2}\{\exp(i\omega_r\tau)(S_z + iS_y) - \exp(-i\omega_r\tau)(S_z - iS_y)\}\right]. \qquad [A5]$$

With the operator $Q = I_x$, and by substituting Eqs. [A4] and [A5] in Eq. [A3], an expression for $1/T_2$ for spin I can be evaluated as

$$\frac{d\langle I_x\rangle}{dt} = -\frac{J^2}{3}S(S+1)\left\{\frac{T_{1Q}}{1+\omega_r^2 T_{1Q}^2} + \frac{1}{2}\left[\frac{T_{2Q}}{1+(\omega_I-\omega_S)^2T_{2Q}^2} + \frac{T_{2Q}/2}{1+(\omega_I-\omega_S+\omega_r)^2T_{2Q}^2} + \frac{T_{2Q}/2}{1+(\omega_I-\omega_S-\omega_r)^2T_{2Q}^2}\right]\right\}\langle I_x\rangle. \qquad [A6]$$

The first term on the right-hand side of Eq. [A6] arises from terms due to F_0A_0 and those in the square bracket arise from the $q = \pm 1$ part of the random Hamiltonian. T_{1Q} and T_{2Q} are the longitudinal-relaxation and the transverse-relaxation times of spin S, respectively. From Eq. [A6] since $\omega_I - \omega_S \gg \omega_r$, the I-spin transverse-relaxation time is

$$\frac{1}{T_2^I} = \frac{J^2}{3}S(S+1)\left[\frac{T_{1Q}}{1+\omega_r^2T_{1Q}^2} + \frac{T_{2Q}}{1+(\omega_I-\omega_S)^2T_{2Q}^2}\right]. \qquad [A7]$$

The above expression shows that $1/T_2^I$ decreases as ω_r is increased. It may be noted that as ω_r goes to zero the above expression is the same as that given in Chap. VIII of Ref. (*4*). Furthermore, if the condition $\omega_I - \omega_S \gg \omega_r$ is not satisfied (this may happen if this calculation is performed for two homonuclear spins or if an uncoupled spin I relaxes by an external random field), the decay rates of $\langle I_x\rangle$ and $\langle I_y\rangle$ differ (*4*, Chap. XII) and should, therefore, be evaluated separately. However, in the present case, since $\omega_I - \omega_S \gg \omega_r$, the two transverse decay constants are identical and a single T_2 can be defined for the I-spin spectrum.

Note that the contribution from the second term in Eq. [A7] is negligible since $(\omega_I - \omega_S)T_{2Q} \gg 1$, and, hence, the expression for $1/T_2^I$ is

$$\frac{1}{T_2^I} = \frac{J^2}{3}S(S+1)\frac{T_{1Q}}{1+\omega_r^2T_{1Q}^2}. \qquad [A8]$$

Equation [A8] shows that the effect of RF irradiation of spin S to change the frequency of the spectral density from zero to ω_r and the condition for suppression of the linewidth

arising from the scalar relaxation of the second kind is $\omega_r^2 T_{1Q}^2 \gg 1$. The expression for $1/T_2^I$ reported earlier by Browne *et al.* (*23*) differs from Eq. [A8] in that the right-hand side erroneously contained $\omega_r^2 T_{2Q} T_{1Q}$, which resembles a saturation factor, in place of $\omega_r^2 T_{1Q}^2$. It may be stated parenthetically that these two expressions become fortuitously equal if the quadrupolar relaxation of spin S is in the extreme narrowing limit for which $T_{1Q} = T_{2Q}$ (*4*, Chap. VIII). It is also useful to note that the second term on the right-hand side of Eq. [A7] arises from the flip-flop (or $q = \pm 1$) terms in the scalar interaction $\mathbf{I} \cdot \mathbf{S}$, and Eq. [A8] is equivalent to one derived by dropping this term and retaining only the $I_z S_z$ part. The matrix given in Eq. [22], which is computed after dropping the flip-flop term (see Eq. [5]), does not include the negligible contributions to the linewidth arising from this term.

Following the same procedure for the derivation of $1/T_2^I$, it can be shown that (with $Q = I_z$), the expression for $1/T_1^I$ of the I spin is not affected by the decoupling and is given by

$$\frac{1}{T_1^I} = \frac{J^2}{3} S(S+1) \left[\frac{T_{2Q}}{1 + (\omega_I - \omega_S)^2 T_{2Q}^2} \right] \qquad [A9]$$

which is vanishingly small since $(\omega_I - \omega_S)^2 T_{2Q}^2 \gg J^2 S(S+1) T_{2Q}$.

ACKNOWLEDGMENTS

This work is supported in part by NIH Grant GM 43966, and by IUPUI. We are grateful to the referee of the original version for valuable comments which led to a more complete form of the theory presented in this paper.

REFERENCES

1. G. Wagner, *Prog. NMR. Spectrosc.* 22, 101 (1990).
2. S. W. Fesik and E. R. P. Zuiderweg, *Q. Rev. Biophys.* 23, 97 (1990).
3. J. A. Pople, *Mol. Phys.* 1, 168 (1958).
4. A. Abragam, ''The Principles of Nuclear Magnetism,'' Clarendon Press, Oxford/London, 1961.
5. M. Ikura, L. E. Kay, and A. Bax, *J. Am. Chem. Soc.* 29, 4659 (1990).
6. L. E. Kay, M. Ikura, and A. Bax, *J. Magn. Reson.* 89, 496 (1990).
7. P. Schmider, V. Thanbal, L. P. McIntosh, F. W. Dahlquist, and G. Wagner, *J. Am. Chem. Soc.* 113, 6323 (1991).
8. T. Yamazaki, W. Lee, C. H. Arrowsmith, D. R. Muhandiram, and L. E. Kay, *J. Am. Chem. Soc.* 116, 11655 (1994).
9. S. Grezesiek, J. Anglister, H. Ren, and A. Bax, *J. Am. Chem. Soc.* 115, 4369 (1993).
10. J. M. Anderson and J. D. Baldeschwieler, *J. Chem. Phys.* 40, 32441 (1964).
11. Anil Kumar, N. R. Krishna, and B. D. Nageswara Rao, *Mol. Phys.* 18, 11 (1970).
12. A. A. Bothner-By, R. L. Stephens, and Ju-mee Lee, *J. Am. Chem. Soc.* 106, 811 (1984).
13. A. Bax and D. G. Davis, *J. Magn. Reson.* 63, 207 (1985).
14. R. R. Ernst, G. Bodenhausen, and A. Wokaun, ''Principles of Nuclear Magnetic Resonance in One and Two Dimensions,'' Clarendon Press, Oxford/London, 1987.
15. J. Fejzo, A. M. Krezel, W. M. Westler, S. Macura, and J. L. Markley, *J. Magn. Reson.* 92, 651 (1991).
16. C. Zwahlen, S. J. F. Vincent, L. Di Bari, M. H. Levitt, and G. Bodenhausen, *J. Am. Chem. Soc.* 116, 362 (1994).
17. B. D. Nageswara Rao and B. D. Ray, *J. Am. Chem. Soc.* 114, 1566 (1992).
18. L. G. Werbelow and A. Thevand, *J. Magn. Reson. A* 105, 88 (1993).
19. R. E. London, D. M. LeMaster, and L. G. Werblow, *J. Am. Chem. Soc.* 116, 8400 (1994).
20. L. G. Werbelow and R. E. London, *J. Chem. Phys.* 102, 5181 (1995).
21. B. D. Nageswara Rao, *Adv. Magn. Reson.* 4, 271 (1970).
22. H. W. Spiess, ''Dynamic NMR Spectroscopy,'' Vol. 15, p. 55 Springer-Verlag, Berlin, 1978.
23. D. T. Browne, G. L. Kenyon, E. L. Packer, H. Sternlicht, and D. M. Wilson, *J. Am. Chem. Soc.* 95, 1316 (1973).